2023-11-21

On the selection of design waves for predicting extreme motions of a floating offshore wind turbine

Brown, S

10.1016/j.oceaneng.2023.116400
Ocean Engineering
Elsevier

On the selection of design waves for predicting extreme motions of a floating offshore wind turbine

S.A. Brown[a,*], T. Tosdevin[a], S. Jin[a,1], M. Hann[a], D. Simmonds[a], D.M. Greaves[a]

[a]*School of Engineering, Computing and Mathematics, University of Plymouth, Plymouth, United Kingdom*

Abstract

Governments worldwide are setting ambitious targets for renewable energy sources as a response to the ongoing climate crisis, leading to increased investment in offshore wind. While fixed wind structures have restrictive water depth limitations, floating devices are being developed to harness the resource in deeper waters. As part of this development, accurate prediction of ultimate loads and platform motions is crucial for survivability and cost-competitiveness. Present design standards rely on time-consuming methodologies based on irregular sea state data to determine design loads. 'Short design waves' are a potential solution to speed up the process by simulating short wave profiles that target extreme responses, bypassing the need for modelling long-duration irregular sea states. This paper explores the application of short design waves to semi-submersible wind platforms, and aims to determine whether extreme motions produced by these methods are comparable with current design practices. Short design waves show promise for surge and heave extremes, but further refinement is needed to improve pitch predictions and align with industry standards. Based on the present comparison, short design waves have potential within early design stages, where a wide range of environmental conditions are explored, but their reliability and applicability in alternative scenarios requires further investigation.

Keywords:
NewWave, Most Likely Extreme Response, Conditional Random Response Wave, Survivability, Accelerations, Laboratory Testing

1. Introduction

As governments worldwide recognise the potential consequences of the ongoing climate crisis, increasingly ambitious targets for renewable energy sources are being integrated within strategies to reduce greenhouse gas emissions. Offshore wind energy is one renewable source that is currently experiencing considerable expansion and investment to meet these government targets. Fixed offshore wind devices are a well established option, built upon knowledge and expertise from the onshore wind industry, but the number of viable wind farm locations is limited by water depth constraints (typically less than 50 m) due to the supporting structure being installed directly in the sea bed. Since it is estimated that 80% of the global offshore wind resource is located in water depths greater than 60 m (Global Wind Energy Council, 2022), alternative solutions that can be installed in deeper waters would greatly increase the total potential for offshore wind.

Floating Offshore Wind Turbine (FOWT) concepts have potential to address this water depth limitation by installing the tower on a floating platform which is typically kept on station through a mooring system. Recent innovation in this sector has led to a large number of proposed FOWT concepts and, unlike fixed wind equivalents, the industry is still experiencing considerable design divergence (Edwards et al., 2023). Since the devices are expected to operate in harsh environmental conditions, one key consideration for all designs is the survivability of the system, which is complicated by a large parameter space due to a combination of wave-wind-currents and the platform motion. Furthermore, FOWTs are in their infancy compared with fixed wind equivalents (accounting for 0.2% of global offshore wind capacity in 2022 (Global Wind Energy Council, 2022)) and hence the number of case studies are relatively small. Over the last decade the devices that have been deployed can largely be categorised as prototype or demonstrator scale models (Edwards et al., 2023), with only three fully operational floating wind farms at the end of 2022 (Edwards et al., 2023). This has led to relatively short testing periods (compared with the likelihood of an extreme event occurring) and hence there is still significant uncertainty in the ultimate loads that a device must survive at a given site. With the projected expansion of total FOWT capacity (Global Wind Energy Council, 2022) and the number of planned farm scale projects increasing, it is vital that the ultimate loads are predicted accurately and efficiently in order to minimise the risk for investors whilst

*Corresponding author
Email address: scott.brown@plymouth.ac.uk (S.A. Brown)
[1]Present Address: Ocean Institute, Northwestern Polytechnical University, Taicang, Jiangsu, China

Abbreviations

AoM	Average of Maxima
CFD	Computational Fluid Dynamics
CNW	Constrained NewWave
CRRW	Conditional Random Response Wave
EVD	Extreme Value Distribution
FOWT	Floating Offshore Wind Turbine
GPD	Generalised Pareto Distribution
ISS	Irregular Sea State
MLER	Most Likely Extreme Response
MPM	Most Probable Maximum
NW	NewWave
O&G	Oil and Gas
ORE	Offshore Renewable Energy
RAO	Response Amplitude Operator
SDW	Short Design Wave
WEC	Wave Energy Converter

ensuring the technology is cost-competitive. Furthermore, since frequent personnel visits to the wind farm will be required for operations and maintenance purposes, it is important that the maximum platform motions in given environmental conditions can be predicted accurately from a health and safety perspective. Achieving this will help to increase weather windows for these operations, further improving the cost-competitiveness.

International design standards (IEC, 2016; DNV, 2018) presently recommend extremely robust and time-consuming methodologies that utilise short-term Extreme Value Distributions (EVDs) to determine the design loads on a structure, a process which typically requires simulating large quantities of data. A short-term EVD provides the probability of exceedance for the largest responses of a device subjected to particular environmental conditions for a specified exposure time. The recommended exposure time varies depending on the application, but 1-hour is typically used for FOWTs as a compromise between the 10-minute recommendation for a wind condition and 3-hours for the sea state. Based on the anticipated total number of peak loading events within the exposure time, the EVD is obtained by fitting a distribution to the peak events observed in a sample of data (Michelen and Coe, 2015) (the recommended sample size is a minimum of 6-hours for FOWT responses (IEC, 2016; DNV, 2018)). The most rigorous approach for design loads that is recommended by standards is the direct-integration method, which averages short-term EVDs for a large number of sea states within an envelope defined by the environmental characterisation process (Coe et al., 2018a,b). The contour approach is an alternative recommendation (DNV, 2018) which is often more practical since the design load is obtained by selecting a high-percentile value from the EVD containing the largest response from a sample of sea states on an environmental contour associated with a given return period. This significantly reduces the quantity of data required, but is largely still limited to scenarios with linear responses to ensure that low-order, computationally efficient numerical modelling approaches can be utilised reliably. A challenge, however, is that the device responses are often nonlinear, and even the introduction of weakly nonlinear terms can increase the computational cost to such an extent that modelling a large number of sea states is impractical. Should the problem require high-fidelity modelling, a single sea state would likely require more computational resource than the typical designer would have available to them, making current best practice guidelines infeasible. Laboratory testing overcomes this problem to an extent but this resource is time-consuming and limited in availability rendering it extremely expensive from a financial perspective.

Alternative methods that could both determine design loads more efficiently and allow the use of higher-fidelity codes where necessary within the design process, would clearly be highly beneficial. Use of Short Design Waves (SDWs) bypasses the need to model a long-duration Irregular Sea State (ISS) by utilising a short wave profile that is designed to produce an extreme response. In the literature, SDWs are typically used for three purposes: predictions of characteristic loads through short-term EVDs (Taylor et al., 1997); for direct characteristic load predictions (Van Rij et al., 2018; Wang et al., 2021); and to study extreme responses in a generic manner by scaling the wave amplitude to the most probable maximum (Quon et al., 2016). SDWs can consist of a single focused wave group, or a focused wave group embedded within a random irregular wave background, referred to as 'single SDWs' and 'constrained SDWs', respectively.

One example of a single SDW is NewWave (NW), a representation of the most probable extreme wave originally developed by Tromans et al. (1991) through treating the sea state as a Gaussian process. The use of NW for fixed or large floating structures, such as those used in the offshore Oil and Gas (O&G) industry, is common practice due to strong correlation between large waves and extreme loading events. However, previous research has shown that this trend does not necessarily hold for more dynamic floating structures, such as is typical in the Offshore Renewable Energy (ORE) sector, since the history effects are non-negligible (Hann et al., 2018; Jin et al., 2022). Despite this, NW has been utilised in a wider ORE context for survivability (Hann et al., 2015; Ropero-Giralda et al., 2020; Katsidoniotaki et al., 2021) and comparative studies (Brown et al., 2020; Ransley et al., 2020a,b) of Wave Energy Converters (WECs). However, the number of NW studies with

FOWTs are more modest, and typically limited to Computational Fluid Dynamics (CFD) analysis comparing the sensitivity of the devices response for different wave parameters (Lin et al., 2021; Zhou et al., 2021).

An alternative single SDW in the literature is the Most Likely Extreme Response (MLER); a response-conditioned methodology originally developed for assessing extremes of the highly dynamic structures within the maritime sector (Dietz, 2005). In short, the methodology utilises a focused wave that is conditioned via the linear Response Amplitude Operator (RAO) of the response of interest to produce the most likely maximum (Dietz, 2005; Quon et al., 2016). Response-conditioned methods such as this are likely to be of greatest benefit in situations where the dynamic response is large. For very large floating platforms, such as those used in O&G, the response is usually small compared with the size of the structure. Consequently, assuming a stationary structure is reasonable in many O&G applications, and NW is commonly used over response-conditioned methods due to the correlation between the largest wave and extreme events for fixed structures. However, there are a limited number of examples of a response-based method similar to MLER known as the 'NewWave in Response' (Grice et al., 2013) being applied to study green water on Floating, Production, Storage and Offloading (FPSO) structures (Chen et al., 2019). In the context of ORE, response-conditioning could be a useful tool due to the more dynamic structures often considered in these applications. Hence, the MLER method has previously been demonstrated through CFD simulations for WEC applications (Coe et al., 2019; Van Rij et al., 2019), although the results exhibited significantly smaller responses than those obtained from the long-duration ISSs recommended by standards for these devices (Rosenberg et al., 2019). Jin et al. (2022) used MLER to predict extreme relative pitch angles of a floating hinged-raft WEC through a physical modelling approach, showing reasonable agreement with ISS data under certain hydrodynamic conditions. In the context of FOWTs, however, the literature for MLER is quite limited with the only previous application presented by Tosdevin et al. (2022) as part of the same physical campaign as that presented in this work, to the best of the author's knowledge.

Previous research on SDWs for floating ORE devices has indicated that history effects are particularly important in generating extreme events (Hann et al., 2018; Jin et al., 2022). This provides the motivation for constrained SDWs, where the focused wave is embedded within a background wave, typically a short sample of an ISS. Constrained NewWave (CNW) (Taylor et al., 1997), which uses NW for the embedded wave, has been investigated for point-absorber type WECs (Göteman et al., 2015; Hann et al., 2018), reporting high variation in the maximum loads between background wave seeds. The Conditional Random Response Wave (CRRW), the constrained equivalent of MLER, has also been demonstrated by Jin et al. (2022) to provide larger mooring loads and pitch angles for a hinged-raft WEC than the single SDW equivalent. Furthermore, the observed loads were shown to be in line with ISS data in certain scenarios, although large variation between different background wave seeds implies that optimised seed selection could be beneficial (Jin et al., 2022). Tosdevin et al. (2021) also demonstrated the CRRW approach for the Mocean WEC, noting that the observed loads were in line with present design standards in a relatively benign sea state. In the context of FOWTs, however, the literature is sparse for constrained SDWs, and is limited to CRRW runs by Tosdevin et al. (2021) as part of the present physical campaign, to the best of the author's knowledge. With the recent introduction of CNW within industry standard codes (Wang et al., 2022), the use of SDW within the design process is more readily accessible to developers than ever before. However, if SDWs are to be incorporated within best practice guidelines for FOWT design, it is necessary to address the knowledge gap in the literature, especially as it is unclear whether the conclusions from WECs are directly transferable due to differences in the typical motions of the two applications.

The present study considers the application of SDWs to a semi-submersible FOWT through a 1:70 scale physical modelling campaign conducted at the Coastal, Ocean And Sediment Transport (COAST) Laboratory at the University of Plymouth, UK. The paper aims to address the SDW knowledge gap in the FOWT literature by considering: 1) whether SDWs are able to produce extreme values that are comparable with present design practices; 2) the relative performance of each SDW for this application; and 3) whether the constrained results can be potentially improved by pre-selecting the background wave based on information known *a priori*. The device is, therefore, examined for 1-hour ISSs and four SDW approaches: NW; CNW; MLER; and CRRW. The work primarily focuses on the device's motion, including velocities and accelerations. These parameters can be useful for multiple reasons

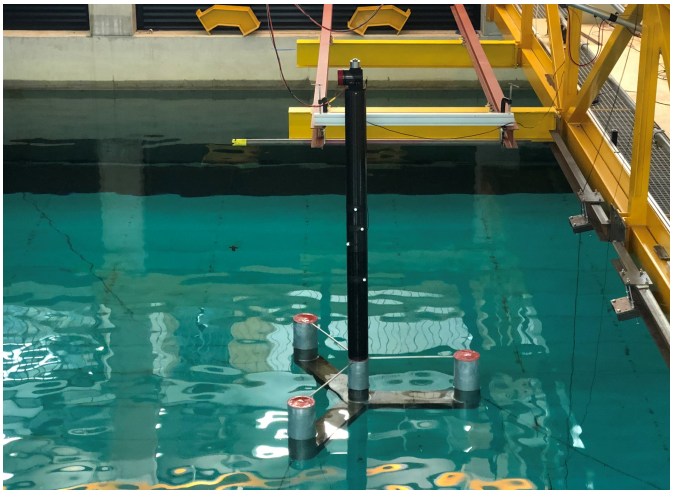

Figure 1: The 1:70 scale model of the VolturnUS-S used in this study.

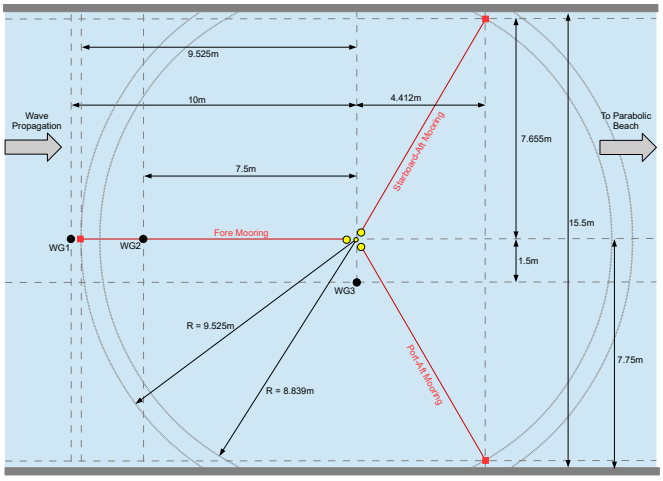

Figure 2: Experimental setup of the FOWT model in the COAST Laboratory. The anchor points for the moorings (red squares) and wave gauges (black circles) are also presented.

		Model 1:70	Model 1:1	Reference 1:1
Mass	[kg]	56.23	1.929e+7	1.994e+7
Draft	[m]	0.286	20.0	20.0
X_{CoG}	[m]	-0.0005	-0.034	-0.300
Y_{CoG}	[m]	0.000	0.000	0.000
Z_{CoG}	[m]	-0.0241	-1.690	-2.140
$\mathbf{I}_{xx}$	[kg·m^2]	26.550	4.462e+10	4.453e+10
$\mathbf{I}_{yy}$	[kg·m^2]	26.551	4.462e+10	4.446e+10
$\mathbf{I}_{zz}$	[kg·m^2]	14.120	2.373e+10	2.388e+10
$f_{n,X}$	[Hz]	0.0679	0.0081	0.007
$f_{n,Z}$	[Hz]	0.4049	0.0484	0.049
f_{n,R_y}	[Hz]	0.285	0.0341	0.036

Table 1: Mass properties of the FOWT model at laboratory (1:70) and full (1:1) scale, relative to the reference device. Moment of inertia ($\mathbf{I}$) is provided relative to the centre of mass. Natural frequencies are presented for surge ($f_{n,X}$), heave ($f_{n,Z}$) and pitch (f_{n,R_y}). All scaling has been achieved using Froude similarity principles.

including as a proxy for mooring or dynamic power cable loading, which have dependence on maximum surge extension; survivability of turbine blades, which is linked with pitch accelerations; stability of the platform to influence design conditions; and worst case scenarios in benign sea states which can affect operation and maintenance.

The paper is structured such that Section 2 establishes the experimental case study, environmental test conditions and SDW approaches considered; Sections 3 and 4 present the results for the short-term ISSs and SDWs; Section 5 discusses the potential of the SDW approaches and the research direction for future work. Finally, conclusions are drawn in Section 6.

2. Physical Modelling Campaign

Experiments are conducted in the Ocean Basin at the COAST Laboratory at the University of Plymouth, UK. The facility is 35 m in length, 15.6 m wide and has an adjustable floor to allow for a range of operating water depths up to a maximum of 3 m.

2.1. FOWT Model, Setup and Instrumentation

The physical model utilised in this work is a 1:70 scale model of the IEA-15-240-RWT and VolturnUS-S platform (Figure 1), developed based on the IEA Wind Task 37 reference documents (Allen et al., 2020; Gaertner et al., 2020). The mass properties of the platform are adjusted to account for fresh water, ensuring a consistent platform draft with respect to the reference device (Table 1). As specified in the reference document for the platform (Allen et al., 2020), a 3-point catenary chain mooring system is utilised for station-keeping, and the operational water depth is set to 2.86 m (200 m at full-scale). Following Froude similarity principles, the mooring system is scaled such that it is consistent with the reference model (Allen et al., 2020). However, due to constraints imposed by the size of the wave basin the moorings are truncated, with the line lengths and anchor locations modified accordingly (Figure 2). Preliminary numerical simulations using a cable dynamic software (Palm et al., 2017) have verified that these truncated moorings will not be fully suspended within the expected range of motion of the FOWT. Hence, minimal discrepancy is anticipated with respect to the full untruncated mooring system.

In the cases with wind loading on the turbine, a thruster system is utilised to apply a constant axial loading at the top of the tower (Ransley et al., 2023), providing an offset in the equilibrium position of the device. This simplified representation has clear limitations due to missing dynamic coupling between the aerodynamics and the platform motion, including neglecting gyroscopic effects on the turbine which can lead to coupling in all six degrees of freedom (Tang et al., 2021). However, in order to model these effects a sophisticated hybrid testing system with motion feedback and multiple rotors would be required. Development of such a system is outside of the scope of the present study. Hence, since the present focus is on the hydrodynamic forcing, inclusion of mean aerodynamic effects is considered a reasonable initial step.

The motion of the device is measured using a Qualisys optical tracking system calibrated to track using a right-hand coordinate system defined such that positive x is in the direction of wave propagation; y is the transverse horizontal component; and z is the vertical dimension. Three resistance wave gauges are utilised to record the wave elevation (Figure 2), with the data obtained from the gauge in line with the equilibrium position of the device (WG3) reported in this work.

2.2. Environmental Conditions

The environmental conditions are derived from a potential FOWT deployment site off the coast of Maine, USA (Viselli et al., 2015). Two design scenarios are investigated: a hydrodynamic survival condition where the turbine is idling but the device is subject to a 50-year sea state; and an operational condition where the turbine is near the rated wind speed (i.e. large turbine loading) whilst the device is in an operational sea state. These scenarios are considered to be similar to design load cases DLC-6.1 and DLC-1.6 in the International Electrotechnical Commission (IEC) standards, respectively. Details of the two conditions are given below, with key parameters summarised in Table 2. Note that the aim of this work is to demonstrate the performance of SDWs relative to current design practices, rather than to provide the most extreme responses for the device. Since identifying the environmental conditions that lead to these largest extremes is non-trivial (Haselsteiner et al., 2021), this is not considered within the scope of the present study and the chosen scenarios are simply intended to be representative examples that demonstrate SDW capabilities.

2.2.1. Hydrodynamic Survival Scenario

A 50-year return contour is determined by fitting a joint distribution to 30 years of hindcast data for mean wind speed (U), significant wave height (H_s) and peak wave period (T_p) from the European Centre for Medium-Range Weather Forecasts (ECMWF) (Hersbach et al., 2018). Utilising an existing approach (Li et al., 2013), U is selected as the marginal distribution, with the joint distributions $H_s|U$ and $T_p|H_s|U$ calculated respectively. The sea state investigated in this scenario is selected as the peak of the 50-year return period contour (for a wind speed of $U = 37\,\mathrm{m/s}$), namely, $H_s = 12\,\mathrm{m}$ and $T_p = 14.4\,\mathrm{s}$. Since the turbine is considered to be in an idling state, and neglecting wind loading on the tower, no aerodynamic force is applied in this scenario. These environmental parameters are summarised in Table 2.

2.2.2. Operational Scenario

A slice of the 3D contour at the rated wind speed is taken and several sea states along it studied. The operational sea state presented here is the one found to produce the largest responses, namely, a sea state with $H_s = 5.95\,\mathrm{m}$ and $T_p = 9\,\mathrm{s}$. This information is summarised in Table 2.

Scale	Case	U [m/s]	F [N]	H_s [m]	T_p [s]	h [m]
1:1	Surv.	37	0.00	12.0	14.4	200
	Oper.	10.59	1.6e+6	5.95	9.00	200
1:70	Surv.	4.42	0.00	0.171	1.72	2.86
	Oper.	1.27	4.78	0.085	1.08	2.86

Table 2: Environmental conditions for the two scenarios, Operational (Oper.) and Hydrodynamic Survival (Surv.): U is the theoretical wind speed; F is the target force for the thruster. The parameters are presented at full and model scale, according to Froude similarity. A JONSWAP spectrum is assumed in all cases, with $\gamma = 3.3$.

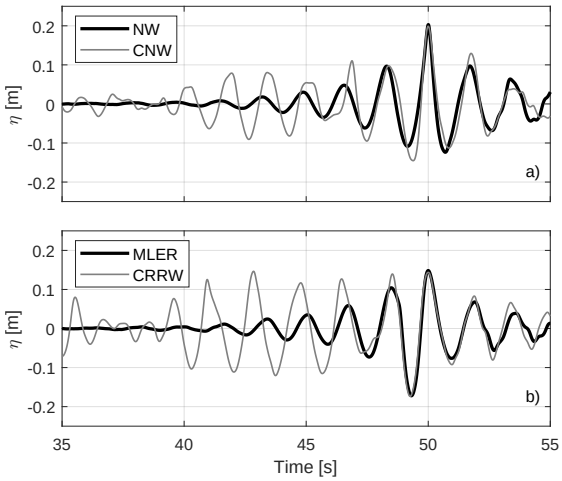

Figure 3: Example SDW profiles recorded at WG3 for the hydrodynamic survival scenario: a) NW and CNW; b) MLER and CRRW, conditioned on negative pitch angle.

2.3. Short Design Waves

In this study, four SDW methodologies are evaluated, derived from the wave conditions identified in Section 2.2. Two single SDWs are considered (NW and MLER) along with the constrained equivalents (CNW and CRRW, respectively). Since the derived equations for each method are quite involved, they are omitted here for brevity. For further details including equations, the reader is referred to Tromans et al. (1991) for NW; Taylor et al. (1997) for CNW; and Dietz (2005) for MLER and CRRW. Examples of recorded SDW profiles are presented in Figure 3. The main peak of each SDW occurs at 50 s (Figure 3), with the constrained waves embedded within a 60 s random ISS and tested for at least 15 different seeds. The response-conditioned SDWs are generated using the RAOs of the device, obtained using 1-hour ISSs with varying random seeds for the phases. This 1-hour ISS data is also used as the benchmark for the SDW analysis throughout.

2.3.1. Wave-Profile Scaling

SDW amplitudes are commonly taken as the Most Probable Maximum (MPM) values corresponding to the peak of the probability density function (PDF) (Figure 4a). Previous work, however, has shown (Tosdevin et al., 2021, 2022) that due to the importance of history effects this amplitude needs to be inflated to avoid under-prediction and produce a characteristic value in line with traditional irregular wave methods. Hence, a value at the 99^{th} percentile of the cumulative distribution function (CDF) is used in this study, since this has been found to produce reasonable results for other dynamic floating ORE devices (Figure 4a) (Tosdevin et al., 2021, 2022). A comparison of the target NW profile

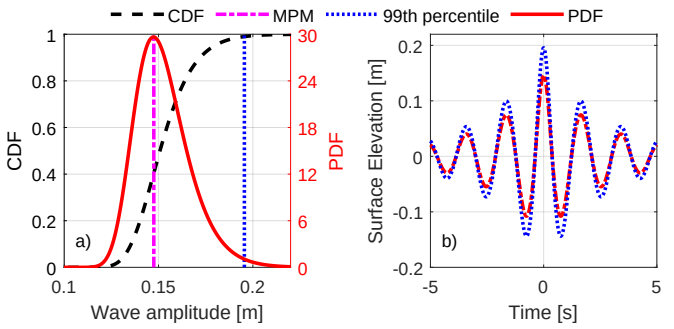

Figure 4: Comparison of different wave scaling methods: a) the definition of the most probable maximum (MPM) and 99$^{\text{th}}$ based on the PDF and CDF, respectively; and b) an example of the target hydrodynamic survival NW profile with each scaling.

with the MPM and inflated percentile is illustrated in Figure 4b for the hydrodynamic survival scenario. Note that in the derivation of the theoretical target wave-profiles, both the wave and response time series are treated with linear theory assuming random Gaussian processes which lead to Rayleigh distributed peaks. A consequence of this for the response-conditioned methods is that the true non-linear response must be a small perturbation of the linear prediction in order for the method to be valid.

2.3.2. Potential Time Savings

One of the key advantages of using SDWs to determine design loads is the substantial time savings compared with traditional methods based on ISS data. Table 3 presents potential time savings based on the typical number of runs that would be required to obtain a design load. The values are given relative to running six 1-hour ISSs, which is the present recommendation in many standards. All of the SDW approaches offer a considerable time saving, with the best case scenario being that the single NW profile provides acceptable characteristic values for all responses of interest (43× faster than ISS). Otherwise the MLER would also provide substantial savings, although it is worth noting that each run would only target a single response and hence the exact time savings would depend on the number of responses of interest. Both constrained approaches offer reduced time savings (≈ 7× faster) due to the requirement of having multiple runs, but would still be beneficial within the design process. Note, however, that the CRRW profiles only target a single response, and hence there are diminishing returns on these time saving benefits as the number of responses increases.

	Run length [s]	# of runs [-]	Total time [s]	Speed up [-]	Responses targetted [-]
ISS	3600	6	21600	-	All
NW	500	1	500	43.2	All
CNW	500	6	3000	7.2	All
MLER	500	1	500	43.2[a]	1
CRRW	500	6	3000	7.2[a]	1

[a]Value for a single response. Divide by total responses of interest for total speedup.

Table 3: Comparison of speedup of each method relative to an ISS result calculated using 6 1-hour simulations. All values provided at full scale. 'Run length' represents the duration simulated within an individual simulation. 'Number of runs' is set to the number of simulations that would typically be run to obtain design loads with each method. 'Total time' is the duration simulated over all the runs (i.e. run length × number of runs). 'Speedup' is (ISS total time) / (SDW total time). 'Responses targetted' is the number of responses that can be evaluated from one instance of the method.

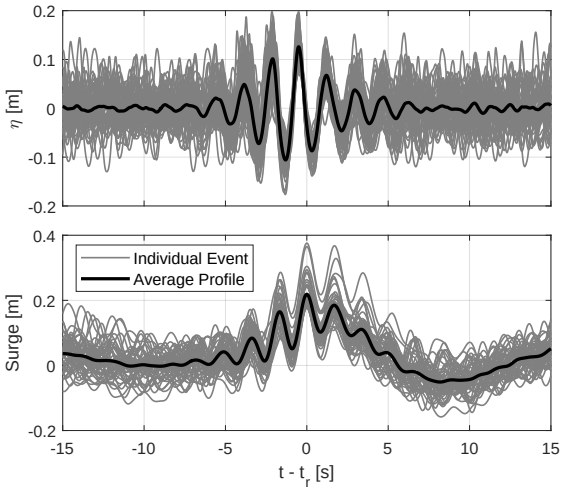

Figure 5: Example of the calculation for empirical wave profiles (surge in the hydrodynamic survival scenario). The grey lines present time series for the largest 50 surge responses (b) observed in the 1-hour irregular wave data, and the corresponding wave leading to these events (a), both aligned by maximum response time (t_r). The black line indicates the average of these events, and this wave profile is referred to as the 'empirical wave profile' throughout this work.

Another consideration when assessing the time savings is the time taken to compute the SDW profiles. In general this calculation can be considered negligible (on the order of seconds), although the response-conditioned methods do require the RAO of the response. This is often available but if not then an ISS simulation is required to obtain this information, which reduces the speed up benefit slightly.

2.4. Data Processing

2.4.1. Spectral Analysis

The spectra, and subsequent RAOs, utilised in this work are calculated using all of 1-hour irregular wave runs for a specific sea state. The spectra are calculated via the Welch's power spectral density estimate using a Hamming window of length 2000.

2.4.2. Average Empirical Profiles

The empirical wave profiles, i.e. the average wave profile that lead to the largest response, are determined using the 1-hour irregular wave data recorded at wave gauge WG3 (Figure 2). The largest n responses occurring within

all of the available data (i.e. all wave seeds) are identified, and are aligned such that the time of maximum response occurs at $t = t_r$. The empirical wave profile is then assumed to be the average of the surface elevation time series for these n events, and is limited to the range $t_r \pm 15\,\mathrm{s}$ (Figure 5). The number of events is set as $n = 50$ in this work, following a preliminary study which suggested that the empirical wave profile is relatively insensitive to this parameter.

2.4.3. Extreme Value Distributions

The EVDs presented in this article are calculated using all of the 1-hour irregular wave runs for a specific sea state. The peak distribution is first obtained by fitting a Generalised Pareto Distribution (GPD) to the empirical data utilising a peak over threshold method, with the threshold specified as the 90^{th} percentile (DNV, 2018). This peak distribution provides the probability of a single peak response being less than a given response magnitude in a specific sea state.

The EVD, on the other hand, provides the non-exceedance probability, defined as the probability that a particular response value, Ψ, is not exceeded within a specified exposure time, set to 1-hour in the present work. The EVD is obtained by considering the total number of peak events, n_p, within the exposure time, and determining the probability that each of these events is less than Ψ. This is equivalent to the product of the peak distribution n_p times, i.e. for a specific response type ψ, the EVD would be determined from the peak distribution (PD) through

$$\mathrm{EVD}(\psi \leq \Psi) = \prod_{i=1}^{n_p} \mathrm{PD}(\psi \leq \Psi) = \mathrm{PD}(\psi \leq \Psi)^{n_p}. \quad (1)$$

In this work, n_p is estimated by a Gaussian process based on the spectral moments, m_k, of the device response (Ochi, 1998),

$$n_p = \frac{1}{4\pi}\left(\frac{1+\sqrt{1-\epsilon^2}}{\sqrt{1-\epsilon^2}}\right)\sqrt{\frac{m_2}{m_0}}, \quad (2)$$

where ϵ is the bandwidth parameter.

2.4.4. Irregular Sea State Benchmarks

Two established methods currently recommended within international standards are presented as a benchmark for the SDWs. The first method, referred to throughout as the 'high-percentile range', is defined as the 75^{th} to 90^{th} non-exceedance percentile obtained from the EVD. The second approach is the average of the maximum responses from each individual 1-hour seed, which will be referred to as the 'Average of Maxima (AoM)' in this study.

3. Irregular Sea States

This section presents results obtained using the 1-hour ISS data, using methodologies consistent with current recommendations in international design standards. The general behaviour of the device during extreme events is discussed here, with the results acting as a benchmark for comparison with the SDWs which are discussed in Section 4.

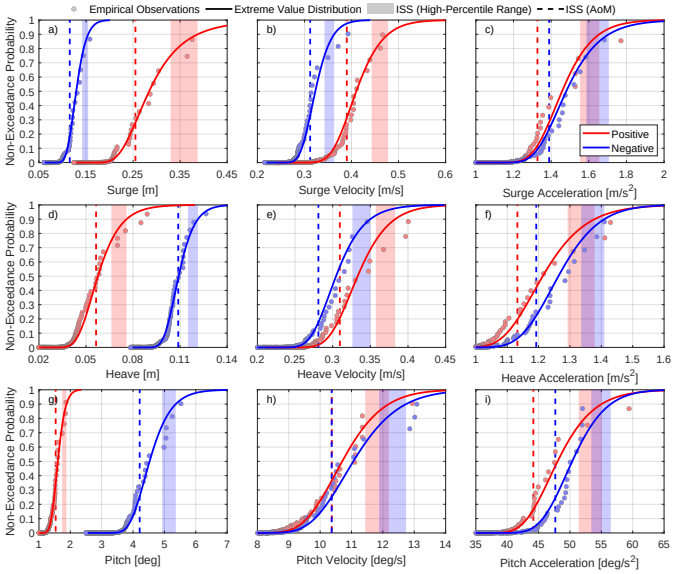

Figure 6: Extreme Value Distributions for different responses in the hydrodynamic survival scenario. The markers represent the observed peaks in the ISS data; the solid lines the EVD; the dashed line is the AoM; and the shaded region is the high-percentile range. The positive direction is presented in red, and negative in blue.

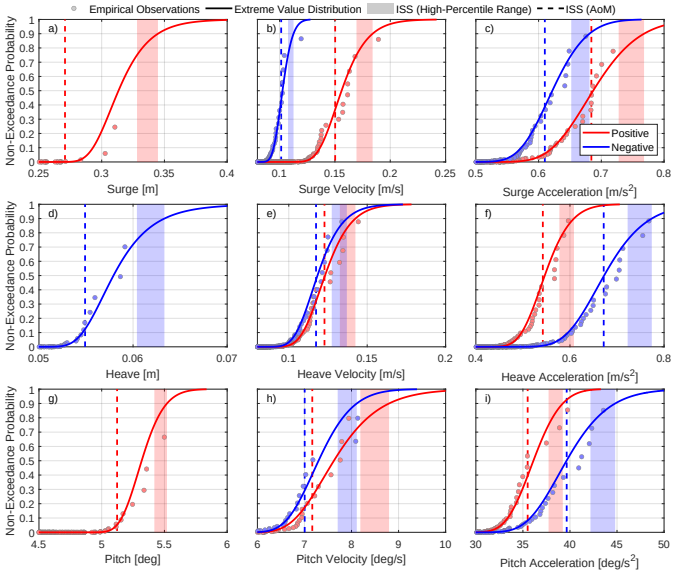

Figure 7: Extreme Value Distributions for different responses in the operational scenario. The markers represent the observed peaks in the ISS data; the solid lines the EVD; the dashed line is the AoM; and the shaded region is the high-percentile range. The positive direction is presented in red, and negative in blue.

3.1. Extreme Value Distributions

Figures 6 and 7 present the EVDs for the hydrodynamic survival and operational scenarios, respectively. The surge (top row), heave (middle row) and pitch (bottom

row) displacement (left column), velocity (middle column) and acceleration (right column) are presented. The observations (circles) and fitted distributions (solid lines) in the positive direction for each variable are presented in red, and the negative direction in blue. The shaded regions indicate the high-percentile range, whereas the dashed lines show the AoM result.

In the hydrodynamic survival scenario (Figure 6), it is observed that there is considerable differences between the magnitude of the positive and negative EVD for each of the three motions. For the surge motion (Figure 6a), the positive EVD is larger and exhibits a considerably longer tail. This extended tail indicates that there are a small number of isolated events where much larger surge responses are observed, which leads to increased uncertainty regarding the maximum loading and, consequently, a wider design load range. In comparison, the largest responses in the negative surge EVD are similar in magnitude, leading to a short tail, and hence a narrow design load range.

The large positive surge offset events lead to increased fore mooring loads, which both pulls the device down and leads to increased negative pitch and heave. In the absence of wind loading, as in the present scenario, this leads to larger negative heave and pitch events than observed in the positive direction (Figure 6g). In common with the observations for surge, the negative pitch EVD has a long tail, which is likely due to the surge-pitch coupling in this problem.

The velocity and acceleration EVDs tend to exhibit smaller disparities between the positive and negative directions, in both magnitude and length of the tail. However, the surge velocity (Figure 6b) is an exception, with the positive direction having larger magnitude. Interestingly, the surge acceleration EVDs show very little difference between the two profiles, suggesting that there are longer phases of positive surge which lead to the extreme surge motions.

The operational scenario exhibits different characteristic extreme behaviour from the hydrodynamic survival scenario. The most notable is that the largest pitch extremes occur in the positive direction due to the mean offset caused by wind loading on the turbine (Figure 7g). In fact, the pitch and surge rarely, if ever, become negative in this particular scenario and hence these EVDs are omitted. The tails of the distributions are quite long, which could in part be due to uncertainty in the GPD fit for this scenario, since there is a reduced quantity of data; i.e. only 9-hours of data is available compared with the 18-hours presented for the hydrodynamic survival scenario. This affects the surge in particular, since the lower frequency of this response leads to fewer events occurring within the sampling period. Note that the presented 9-hours of data is greater than the 6-hour recommendation in many international standards (IEC, 2016; DNV, 2018). This raises questions on the accuracy of the present recommendations especially as maximum surge extension is an important consideration for key components of all FOWT systems including the moorings and dynamic power cables. This is acknowledged to an extent through increased safety factors for moorings, but it also highlights the potential benefits a reliable SDW approach that targets specific extreme responses could provide.

As observed in the hydrodynamic survival scenario, the heave and pitch velocity EVD profiles (Figure 7e,7h) show similarities between the positive and negative directions. The positive surge velocity EVD is considerably larger than the negative, most likely due to the negative velocity phases being reduced by the wind loading. In contrast to the hydrodynamic survival scenario, the acceleration EVDs do show a dependence on direction for all three motions. The positive surge response exhibits larger extremes (Figure 7c) since it is assisted by the wind loading, whereas the negative response is acting against this loading. Conversely, in the heave and pitch accelerations, the negative response is observed to dominate the extremes. For the pitch, this is a little surprising since the negative direction is acting against the wind loading, possibly indicating that the moorings are dominating this response.

3.2. Sensitivity of Established Design Load Methods

Since the established recommended practices using the 1-hour ISSs are being considered as the benchmark for the SDW in this study, it is important to consider the sensitivity of these approaches. Firstly, the sensitivity to the quantity of data is investigated. International standards typically recommend at least 6-hours of data to provide the characteristic response/load (IEC, 2016; DNV, 2018), and in this study considerably more data (18-hours) has been simulated for the hydrodynamic survival scenario. Therefore, Figure 8 presents the surge (a) and negative pitch (b) EVD (solid line) obtained with 6-hours (seeds 1-6; blue), 12-hours (seeds 1-12; red) and 18-hours (seeds 1-18; green) of data, along with the high-percentile range (shaded) and AoM result (dashed line) in the corresponding colour. The EVDs, and consequently the high-percentile range derived from them, vary significantly for the different number of seeds particularly for the surge response. This raises concerns regarding the reliability of the high-percentile method, and this uncertainty is accounted for through more conservative safety factors (DNV, 2018), ultimately leading to over-engineering of FOWTs and hence a sub-optimal cost competitiveness. The AoM method varies less for both responses. This clearly improves the confidence in the result, but it is noted that the design load is considerably less conservative, potentially incurring cost implications due to the increased chance of failure for devices.

The large variability in the results for different quantities of data also raises further questions regarding the suitability of the minimum recommendation of 6-hours of data. Figure 9 presents the EVD for three different 6-hour samples from the 18-hours available (trivially selected as seeds 1-6 (cyan), 7-12 (magenta) and 13-18 (orange)). For both responses the variation in the EVDs is very large;

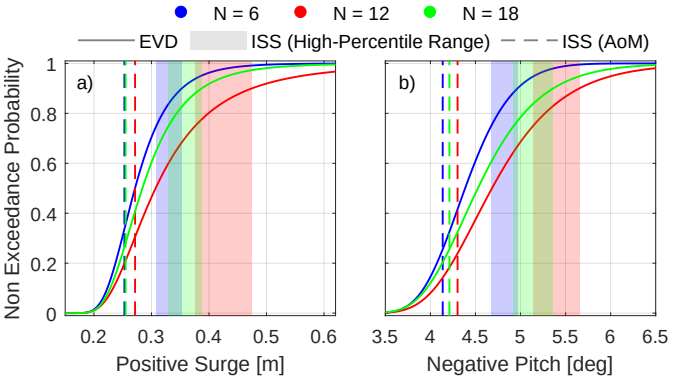

Figure 8: Sensitivity of the EVDs to the number of seeds used in the calculation: six (blue); twelve (red); and 18 (green). Surge (a) and negative pitch (b) from the hydrodynamic survival scenario are presented. The solid lines are the EVDs; dashed lines are the AoM result; and shaded regions are the high-percentile ranges. Note that six seeds is the minimum recommendation by current standards.

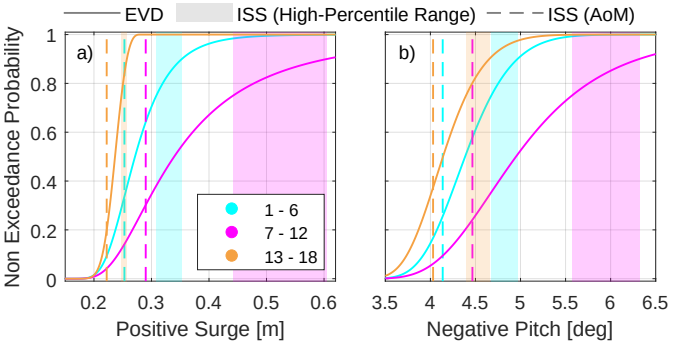

Figure 9: Sensitivity of the EVDs to different sets of six seeds used for the calculation: seeds 1-6 (cyan); seeds 7-12 (magenta); and seeds 13-18 (orange). Surge (a) and negative pitch (b) from the hydrodynamic survival scenario are presented. The solid lines are the EVDs; dashed lines are the AoM result; and shaded regions are the high-percentile ranges.

for instance, the pitch could be selected as approximately 4.5 deg or 6 deg simply based on the random nature of the data sample collection. Note that the three samples have been selected in a simple manner, and it is likely that an even larger range in possible characteristic extremes could be obtained by selecting the worst case combinations of available seeds. This high dependence on the data sample is likely to be most prevalent in responses which have very large extremes that occur at a low frequency, since this: firstly, increases the likelihood that these events will not occur within the sample; and, secondly, leads to a long-tailed EVD if only a small number of much larger events are captured. The AoM method also shows some variation between the three 6-hour samples, but this is considerably less than observed in the high-percentile range approach. Further work on the sensitivity of present design methods using ISSs will be conducted in the future.

In this study, the AoM method is generally utilised for the benchmark for the SDWs due to the better consistency in the results, and a more like-for-like comparison (i.e. an AoM approach is also utilised for the constrained SDWs).

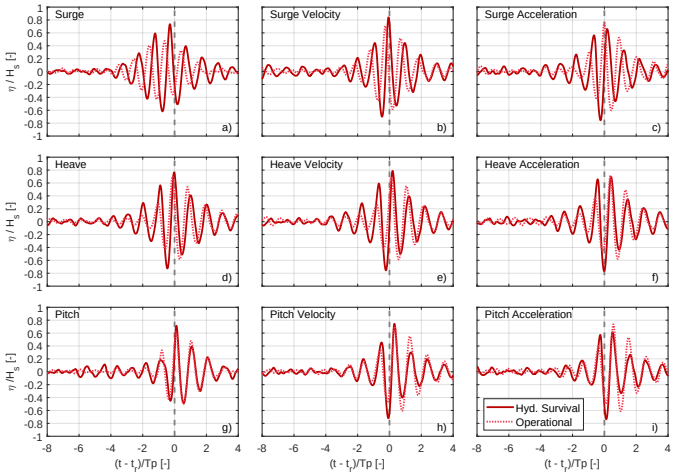

Figure 10: Empirical wave profiles leading to the positive extreme responses. The time axis has been normalised by peak period, and centred around the time of maximum response, t_r. The solid and dotted lines are the hydrodynamic survival and operational scenarios, respectively.

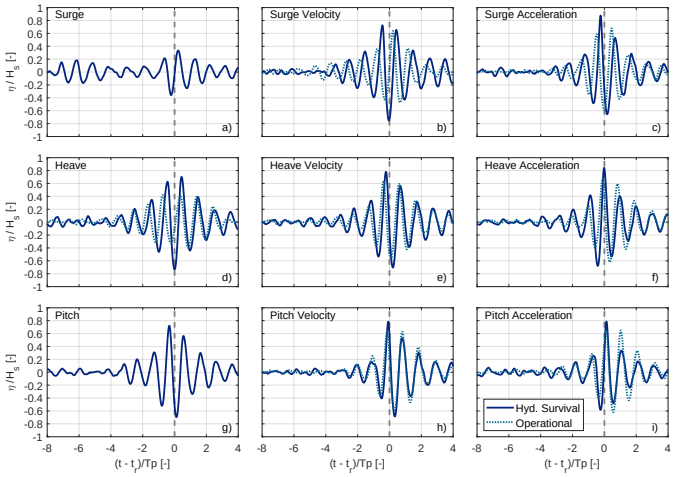

Figure 11: Empirical wave profiles leading to the negative extreme responses. The time axis has been normalised by peak period, and centred around the time of maximum response, t_r. The solid and dotted lines are the hydrodynamic survival and operational scenarios, respectively.

The high-percentile range, where applicable, will also be presented for reference, however.

3.3. Empirical Wave Profiles

Figures 10 and 11 present the empirical wave profiles leading to the positive and negative extreme events, respectively, for each response considered in this study (see Section 2.4.2 for definition). The hydrodynamic survival and operational scenarios are represented as the solid and dotted lines, respectively. Considering the positive extremes first, it is observed that there are similarities between the profiles generated from the different sea states for many of the responses of interest. This may indicate that trends exist in the data which can be transferred to all sea states. The positive pitch (Figure 10g), positive

surge velocity (Figure 10b) and negative acceleration (Figures 11c,11f,11i) profiles exhibit similarities with classical crest focused waves generated with NW theory, such as a single significantly larger peak and relatively symmetrical smaller peaks either side of this event. Hence, one might anticipate that extreme events may be produced by a single crest focused NW for these variables. Some of the other profiles have similarities with NW theory with non-zero phase alignment. For example positive heave acceleration (Figure 10f) looks like a trough focused wave. Other profiles, however, exhibit considerable differences from NW theory. For instance, the average wave profile leading to the positive surge extreme (Figure 10a) in both sea states consists of a series of four progressively larger waves with approximately the peak period of the sea state. In these cases, a single NW profile is expected to be less likely to produce an extreme, and that either constrained waves, to provide history effects, or a response-conditioned SDW would be a more appropriate option.

4. Short Design Waves Results

4.1. NW and CNW

Figures 12 and 13 present the maximum responses for each individual CNW and ISS run for the operational and hydrodynamic survival scenarios, respectively. The AoM is also presented (ISS - solid line; CNW dashed line) along with the NW result (dash-dotted line) and high-percentile range (see Section 3.1). In the operational scenario (Figure 12) CNW provides a larger average prediction than NW for all responses considered in this study, indicating that history effects are non-negligible. For most of these responses, the average of the CNW predictions is also similar to the equivalent from the 1-hour data. This suggests that CNW could potentially be utilised as an alternative to traditional design approaches in this sea state, although the predictions generally fall significantly short of the more conservative high-percentile approach, which essentially utilises a fit to existing data in order to extrapolate to high percentiles. Furthermore, the scaling of the target wave-profile (Section 2.3.1) is conducted such that the extremes are in line with the irregular wave maxima which favours the AoM approach and hence, it is perhaps unsurprising that the CNW data produces a smaller characteristic extreme response than the high-percentile method.

In the hydrodynamic survival scenario (Figure 13), the average of the CNW runs provides a larger response than NW for all positive responses and most negative variables. In general, NW does not provide a good characteristic load, contrary to the hypothesis drawn from the empirical wave profiles (see Section 3.3). However, for the negative surge and surge acceleration responses NW produces a significantly larger result that exceeds the ISS results and almost falls within the high-percentile range. Considering the negative surge empirical wave (Figure 11a),

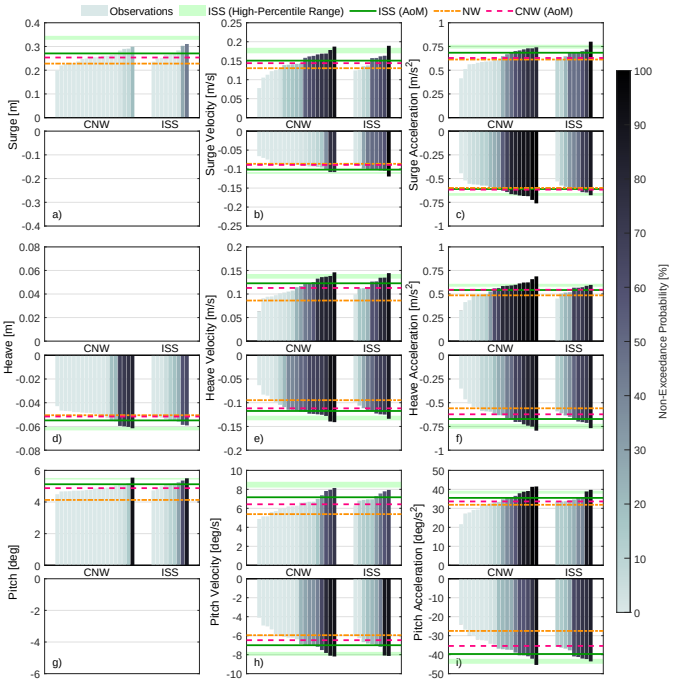

Figure 12: Comparison of maximum responses from the CNW runs with the 1-hour ISS seeds for the operational scenario. The average maxima of these CNW runs (dashed lines) is presented, along with the NW prediction (dash-dotted line) and present recommendations in international standards based on the ISS data: AoM (solid lines) and high-percentile range (shaded regions). The colour of the bar represents the non-exceedance probability.

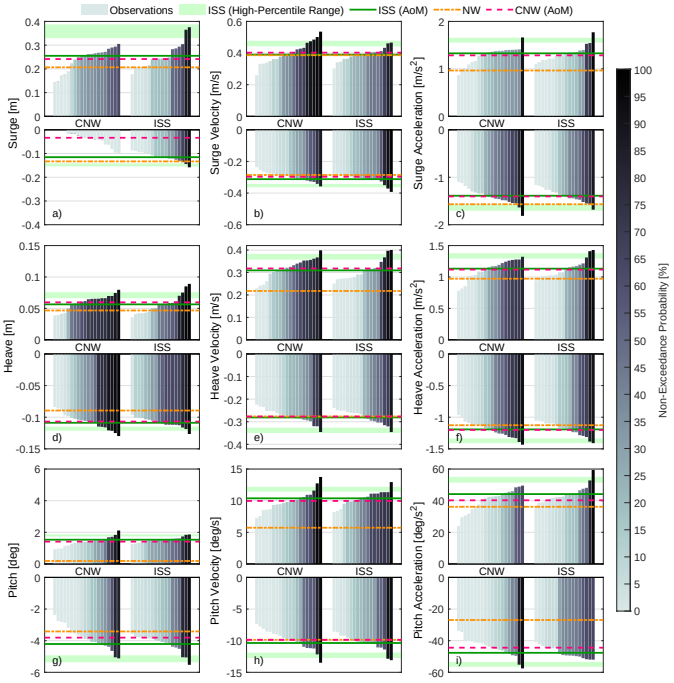

Figure 13: Comparison of maximum responses from the CNW runs with the 1-hour ISS seeds for the hydrodynamic survival scenario. The average maxima of these CNW runs (dashed lines) is presented, along with the NW prediction (dash-dotted line) and present recommendations in international standards based on the ISS data: AoM (solid lines) and high-percentile range (shaded regions). The colour of the bar represents the non-exceedance probability.

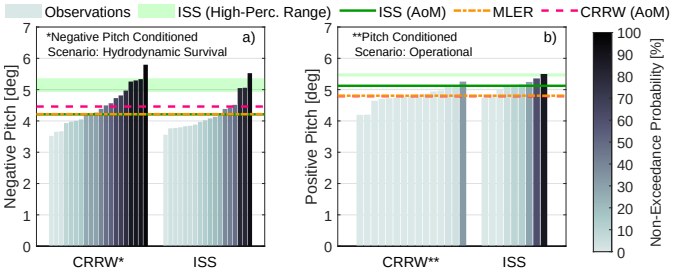

Figure 14: Comparison of maximum responses from the pitch-conditioned CRRW runs with 1-hour irregular sea state (ISS) seeds for the hydrodynamic survival (a) and operational (b) scenarios. The average maxima of these CRRW runs (dashed lines) is presented, along with the MLER prediction (dash-dotted line) and present recommendations in international standards based on the ISS data: AoM (solid lines) and high-percentile range (shaded regions). The colour of the bar represents the non-exceedance probability.

the profile is significantly different from all others in that there is no distinct wave event and this implies that the maxima occurs after a quiet spell of relatively small waves. This, therefore, favours the single SDW, since the preceding waves in the CNW runs cause a positive surge offset prior to the embedded wave occurring. Similar to the operational scenario, the average CNW generally compares well with the average of the 1-hour results, although the pitch related variables (Figure 13g-13i) are consistently underestimated.

Quantifying the success/failure of a method is non-trivial but here a simple percentage approach based on the ISS AoM result is utilised as the benchmark for each response. Table 4 presents the percentage difference, $\mathcal{D}$, for the NW and average CNW prediction. An under-prediction of 10% is considered the minimum threshold for success, and any larger under-prediction is marked in red. Results within 5% of the benchmark are indicated in blue, with very good results ($-2\% \leq \mathcal{D}$) shown in bold. Note that all larger predictions than the benchmark (i.e. positive percentages) are considered very good in this study. The NW method generally fails to satisfy the 10% threshold, often by a large margin, and the only variable that is considered a success in both sea states is negative surge. The CNW results, however, generally show success with many predictions close to or exceeding the benchmark. The failures are generally just short of 10% threshold, which could imply that minor modification of the CNW method through background wave selection or number of runs could potentially lead to successful outcomes for all variables.

4.2. MLER and CRRW

In both scenarios the predictions for the pitch related variables could benefit from improvement since they largely fall in the acceptable category rather than good. One possible improvement could be to utilise response-conditioning approaches such as MLER and CRRW in order to target the extremes in these variables. In this study, response-conditioned approaches are investigated for the pitch in

	Hyd. Survival		Operational	
Response	NW	CNW	NW	CNW
X^+	*-19.00*	-5.34	*-15.85*	-6.38
X^-	**15.43**	*-70.84*	N/A	N/A
$\dot{X}^+$	**-0.94**	**3.23**	*-13.28*	-4.47
$\dot{X}^-$	-8.45	-4.85	*-15.16*	*-12.33*
$\ddot{X}^+$	*-27.24*	-3.20	-10.46	-8.07
$\ddot{X}^-$	**12.95**	**1.05**	**-1.87**	**1.08**
Z^+	*-17.25*	**5.73**	N/A	N/A
Z^-	*-17.80*	**-1.75**	-7.95	-5.98
$\dot{Z}^+$	*-29.67*	**2.75**	*-29.80*	-8.07
$\dot{Z}^-$	**-1.55**	**-1.38**	*-19.39*	-4.75
$\ddot{Z}^+$	*-14.14*	**-1.33**	*-10.37*	**0.48**
$\ddot{Z}^-$	-5.52	**0.71**	*-16.81*	-7.40
R_y^+	*-87.72*	-7.92	*-19.36*	-4.80
R_y^-	*-18.89*	-9.57	N/A	N/A
$\dot{R}_y^+$	*-44.82*	-3.94	*-24.80*	*-10.31*
$\dot{R}_y^-$	-4.92	-4.87	*-15.07*	-7.58
$\ddot{R}_y^+$	*-18.16*	-8.88	*-10.25*	-5.30
$\ddot{R}_y^-$	*-43.48*	-6.78	*-30.67*	*-10.72*

Table 4: Percentage difference, $\mathcal{D}$, of NW and average CNW results compared with the ISS (AoM) benchmark. Red (italic) is unacceptable under-prediction ($\mathcal{D} < -10\%$); black is acceptable ($-10\% \leq \mathcal{D} < -5\%$); blue is a good prediction ($-5\% \leq \mathcal{D}$); bold indicates very good agreement, including larger predictions ($-2\% \leq \mathcal{D}$). Surge (X), Heave (Z) and Pitch (R_y) are presented along with the velocities ($\dot{F}$) and accelerations ($\ddot{F}$). The superscript indicates the positive/negative direction.

the dominant extreme direction for each scenario (negative and positive directions for the hydrodynamic survival and operational scenarios, respectively). Figure 14 presents the pitch-conditioned CRRW and MLER results relative to the 1-hour sea state in the hydrodynamic survival (Figure 14a) and operational (Figure 14b) scenario. In the hydrodynamic survival scenario, the introduction of response-conditioning improves the result considerably, exhibiting $\mathcal{D} = -1.35\%$ and $\mathcal{D} = 5.91\%$ for MLER and CRRW, respectively (compared with $\mathcal{D} = -9.57\%$ for CNW). In the operational scenario, however, the extreme response reduces to $\mathcal{D} = -6.47\%$ compared with $\mathcal{D} = -4.80\%$ for CNW, indicating that response-conditioning may only be beneficial in specific environmental conditions.

4.3. Analysis on Wave-Response Relationships

The constrained SDW methods above show potential with respect to the 1-hour irregular wave data, but the variation exhibited between the individual runs raises questions on whether improvements could be made through the background wave selection process. In this work, the background wave seeds are selected at random, without any prior knowledge on the presented variables, but these results are analysed for trends that could be exploited in

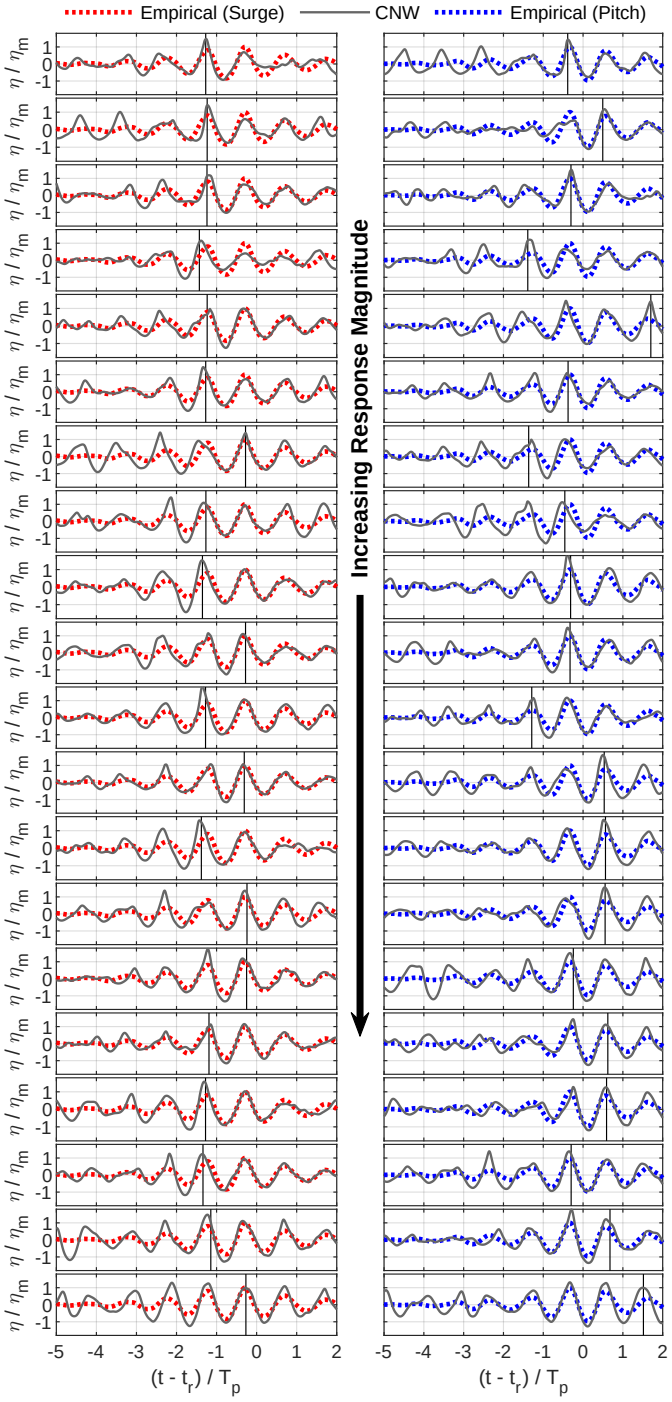

Figure 15: The recorded wave surface elevation (grey line) from each CNW run in the hydrodynamic survival scenario, in ascending order of the magnitude of the response. Surge (left) and negative pitch (right) are presented. The dotted line is the empirical wave profile for each response, and solid vertical line indicates the target time for the main peak of the embedded NW profile. The data is normalised by the maximum recorded in the empirical wave profile.

the future. Note the wave profile is the only known parameter *a priori*, and hence will be the focus of the analysis. However, it is possible that there are relationships between various responses which could be utilised in the future to provide improved response-conditioned approaches. This will be investigated in future work. Due to the large quantity of data available in this study, the analysis is limited to the CNW results for surge and the dominant pitch response in each scenario.

Figure 15 presents the surface elevation profiles (solid line) recorded at WG3 for each of the CNW runs, compared with the surge (left) and negative pitch (right) empirical profile (dotted line). The individual runs have been ordered such that the magnitude of the response is in ascending order. Note that the time axis is relative to the time of maximum response, and the surface elevation axis has been normalised by the maximum of the empirical wave profile (η_m). Comparing with the empirical profiles, the CNW wave profiles for the largest responses appear to have good correlation with the profiles derived from the irregular data in both pitch and surge. Considering the surge profiles, the responses do not generally occur during the main peak of the embedded NW (the theoretical time of occurrence for this peak is indicated by the vertical line). On closer inspection, the main peak of the embedded NW of the largest response is smaller, flatter and more asymmetric than the target profile, and is smaller than the preceding wave. This could imply that wave breaking has occurred, and possibly that the additional drag on the structure, due to the turbulence, is responsible for the largest surge responses. This would increase the parameter space considerably as the largest responses likely depend on the type of breaker (spilling, plunging etc.), and relative position of the occurrence of breaking to the structure. Future work will investigate the sensitivity of this additional parameter space using single SDWs.

In order to determine whether there are any links between the magnitude of the response and the realised wave profile, it is critical to identify the key variables that adequately describe the problem. As an example, a system is defined in this study (Figure 16) where η_0^+ is the last wave peak prior to the maximum response event; η_i^+ and η_{-i}^+ are the i^{th} succeeding and preceding wave peak, respectively; and η_{nw}^+ is the intended peak of the CNW. A similar system is utilised for the troughs (η^-), with the 0^{th} trough considered as the one immediately preceding η_0^+.

Figure 17 presents linear fitting of the maximum surge response against various variables within this defined system, for the hydrodynamic survival (blue points and dotted line) and operational (red crosses and dash-dotted line) scenarios. Considering the CNW peak, η_{nw}^+ (Figure 17a), the data implies that there is a relatively minor relationship between this parameter and the magnitude of the surge. This is consistent with the time series data (Figure 15), which showed that the maximum response times varied considerably in relation to target CNW peak. The data does show moderate correlation with η_0^+ (Figure 17d), implying that a large response does tend to occur following a large peak. The surge magnitude depends less on the preceding waves; there is possible weak correlation on the η_{-2}^+ (Figure 17b) in both scenarios but the hydrodynamic survival scenario shows no correlation with η_{-1}^+ (Figure 17c). In fact, there is similar, if not larger, weak positive cor-

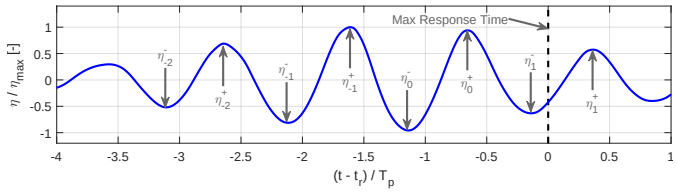

Figure 16: Definition of system used to determine trends within the data.

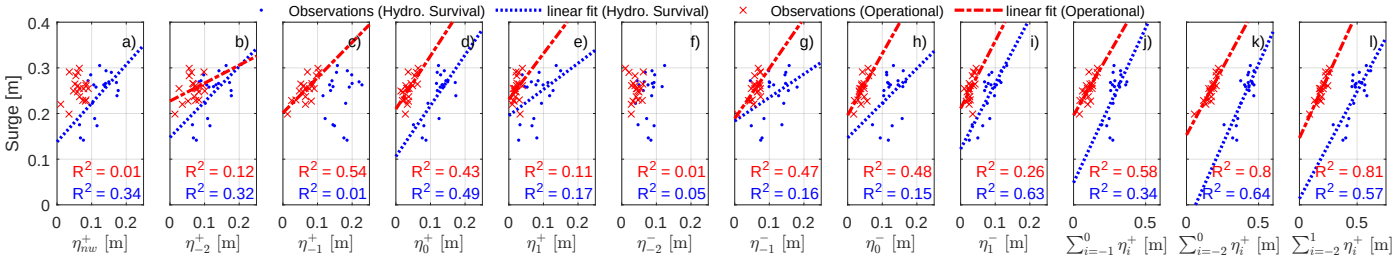

Figure 17: Relationship between the maximum surge response in each CNW run and various parameters relating to the recorded wave elevation. η_i^+ and η_i^- are peaks and troughs, respectively. In cases where R^2 (indicated at bottom of each plot) exceeds 0.1, a linear fit is plotted. The hydrodynamic survival (dots; dotted line) and operational (crosses; dash-dotted line) scenarios are both presented.

relation with η_1^+, implying that the largest responses may be obtained within a series of large waves but it is not necessarily reliant on the size of a single peak. This is further reinforced by considering the summation of the individual peaks (e.g. $\eta_{-1}^+ + \eta_0^+$), which shows increasing correlation as more peaks around the maximum response are included (Figures 17j-17l).

These relationships provide an example of a possible method that could be deployed when selecting the background waves for the surge response in the future. By considering a range of theoretical wave profiles and selecting the ones where the embedded NW occurs within a sequence of large waves, it may be that large characteristic extremes can be obtained more reliably, reducing the number of runs required and/or the confidence in the result. The lack of correlation with the CNW peak suggests that the results are not reliant on perfectly achieving the NW profile, and, based on the wave profiles in Figure 15, it is possible that if the main peak breaks then this could lead to the largest responses. However, it is likely that the largest surge responses are driven by further parameters than simply the peak surface elevation. For instance, there is correlation observed between the 0^{th} trough, η_0^-, and the surge response, particularly for the operational scenario (Figure 17h). It is, therefore, possible that a combination of multiple parameters may provide the background wave profiles which have the highest likelihood of producing an extreme surge response. Note that a similar approach has been tested for the pitch response, but there is very little correlation observed with any of the presented variables. It may be that there are relationships with other characteristics within the wave profile, such as wave steepness or rising time, which would be more appropriate option for this particular response.

5. Discussion and Future Work

In general, the constrained SDWs show promise as a tool within the design process for FOWTs, but the full potential of the methods is unlikely to be realised without further refinement and optimisation of the procedures. Indeed, the limitations of the methods and the role they play within the design process cannot be adequately assessed without first maximising their effectiveness. It may be that the time-saving that SDWs offer makes them ideally suited to the early design stage. For example, they could be utilised to identify the key environmental conditions for a specific device by sweeping large parameter spaces in a more efficient manner, with traditional approaches then applied to satisfy the final design load cases. It is worth noting, however, that these traditional methods have some reliance on statistical sampling, and hence are not infallible. For instance, in this study it is shown that considerably different design loads can be obtained within the dataset using EVD approaches (see Section 3.2). The best-case scenario would be that a deterministic single SDW could be developed for each key response to remove all randomness from the procedure. As is presented above (Section 4), the accuracy of the presently available single SDW approaches are generally too poor to be considered as a viable option in the design process. However, an exception is the response-conditioned MLER that achieved the ISS AoM benchmark for pitch in the hydrodynamic survival scenario (Figure 14a), indicating that response conditioning could be useful in certain scenarios. Future work will, therefore, consider MLER conditioned on alternative responses, as well as explore different environmental conditions to determine when response-conditioning is most effective.

Development of more effective single SDW approaches may be possible by identifying trends in the constrained SDW runs. A relatively simple system is presented in

this study (Section 4.3) using the CNW individual runs to demonstrate a relationship between a series of large waves and large surge responses. If further relationships can be identified, it may be possible to derive the single most likely background wave to produce the largest magnitude for each response. Even if a single background wave cannot be identified, it may still be possible to discard those that are unlikely to produce an extreme, or reduce the range of options. Ultimately, further data is required to perform this analysis in future work, and with such a large parameter space for the background wave, this optimisation may lend itself to a machine learning approach (Carleo et al., 2019). However, any method to determine background waves is only really useful if the trends are transferable between devices. A crucial step in future work, therefore, is to repeat the presented analysis on a range of different FOWT platforms of differing types (semi-subs, spars etc.) to determine the level of transferability in any trends.

From a financial perspective, even if background wave selection must remain random then constrained SDWs still have potential cost benefits (Section 2.3.2). Firstly, since the SDW results are similar to the ISS AoM benchmark, they could be utilised to reduce the time-cost within the design process. Alternatively, due to the reduced cost of each individual run, a considerably larger number of seeds could be conducted in order to be more confident in the result. Any increase in confidence could potentially lead to a reduction in safety factors, reducing device cost and improving cost-competitiveness. However, before SDWs can be integrated within international standards there are a number of elements to assess. An optimisation on the number of individual constrained SDWs runs required to obtain specific confidence intervals is a key parameter, since this will help to determine the amount of time-saving that could be achieved. The type of SDW also factors into this optimisation. If response-conditioned constrained approaches have to be utilised for a large number of design loads then there will be diminishing returns in terms of cost-effectiveness since each simulation will only target a single variable. If, however, wave-conditioned approaches can be utilised for the majority of these variables, with specific key responses targetted using response-conditioning then there could be substantial time-savings. Therefore, determining which design loads require response-conditioning is a crucial step in future work. This will be addressed through application of these response-conditioning techniques to other key responses within a wider range of environmental conditions. Another point that must be addressed is the level of accuracy that is required in order for SDW approaches to be considered comparable to traditional methods. One problem is that the traditional approaches are imperfect (see Section 3.2), creating uncertainty in the benchmark for the SDWs. Thoroughly assessing the sensitivity and uncertainty of both traditional approaches and the SDWs is a crucial step in future work, in order to provide a more accurate comparison of the methods. Furthermore, in order to produce characteristic extremes in line with the high-percentile range, a similar distribution fitting approach for the SDWs data should be considered in future work, as has been trialled in the maritime sector (Drummen et al., 2009). Alternative procedures should also be tested such as only selecting the runs with the largest responses and improved background wave selection (see Section 4.3), to attempt to provide a more accurate characteristic extreme, especially as it is observed in many of the responses that the largest events fall within the high-percentile range.

From a modelling perspective, the possible dependence of the surge response on wave breaking (Section 4) highlights a difficulty with considering the present problem using a physical modelling approach; non-linear processes will generally lead to deviations from the target wave profiles, increasing the complexity of the analysis. The non-linearities are further exaggerated here by the inflated percentile scaling of the wave profiles (Section 2.3.1). It is possible that trends could be more effectively identified in the CNW profiles if a lower-percentile scaling is used to minimise complications such as wave breaking. However, since the surge response appears to be sensitive to these non-linearities this would still not provide the full picture. It is worth noting that numerical models are almost exclusively the tools of choice when running design load cases in present design procedures, often with an acceptance that they are utilised outside of their valid range. Therefore, an alternative option would be to repeat the work presented here utilising a numerical approach in future work to ensure the target wave profiles are realised. This produces different issues, however, since lower-fidelity potential flow models, which are the industry-standard, will not accurately capture the non-linearities (Holcombe et al., 2023). For instance, the wave breaking would commonly be accounted for through an empirical formula (such as modifying the drag coefficient using an additional impact force if a wave exceeds a certain threshold (Marino et al., 2011)), or simply avoided by decreasing the wave height to be just below the breaking limit. This has clear practical benefits in computational efficiency, but is inaccurate when assessing a response that is strongly dependent on non-linear parameters. High-fidelity modelling could be utilised to address this, although accurate turbulence modelling under breaking waves is non-trivial (Brown et al., 2016) and is still an area of active research (Li and Fuhrman, 2021), along with their interaction with structures (Li and Fuhrman, 2022). A comparison of the SDW approaches presented in this work using physical and numerical modelling will be considered in future work, including quantification of the magnitude of the discrepancies between the methods.

For the physical modelling approach presented here, further improvements will be assessed in future work. The aerodynamic emulation is one key area that could be improved to allow for a wider range of scenarios to be addressed. In this work, a simplified aerodynamic model is used which applies a constant thrust on the top of the tower, whereas a real-time hybrid testing system that

utilises surrogate modelling approaches to incorporate the motion of the device (Ransley et al., 2022, 2023) would be a more realistic approach. The development of this system allows modelling of a wider range of environmental conditions in the future, including extension to turbulent wind and wind loading on the tower, and will allow the importance of motion feedback to be investigated for the present device.

6. Conclusions

This study presents SDW predictions of extreme motions for a semi-submersible FOWT to assess their potential as a tool within the design process. Traditional design procedures, based on 1-hour exposure-time ISSs, are utilised as the benchmark for the SDW predictions. The single NW approach, which is often the appropriate choice for fixed structures, is shown consistently to under-predict the extreme motions of the FOWTs due to the neglected dynamic history effects. CNW provides predictions in line with the AoM method in current standards for many responses, particularly surge and heave. For the pitch responses, however, the CNW approach generally provides $5-10\%$ under-predictions compared with the AoM of the ISS data. Utilising response-conditioned SDWs improves these pitch predictions in the hydrodynamic survival scenario, with a single MLER being in agreement with the AoM benchmark, and the constrained CRRW approach being considerably more conservative. In the operational sea state, however, this improvement is not observed, instead providing lower responses than the wave-conditioned CNW approach. This inconsistency in the effectiveness of response-conditioning implies that future work should focus on a wider range of environmental conditions and responses in order to determine where SDWs can be used reliably.

All SDW predictions in this study fall short of the more conservative high-percentile approach, which utilises data fitting to extrapolate to high-percentile responses. It may be possible to provide a more like-for-like comparison with the high-percentile range by applying a similar data fitting approach to the SDW data in future work. However, it is shown in this work that the high-percentile range approach is very sensitive to the quantity of data, particularly for variables which have very large responses that occur infrequently. For instance, using three different sets of six 1-hour seeds, the minimum recommended in most standards, considerably different design loads are obtained within the 18-hours of data collected in this study. Future work should thoroughly assess the sensitivity of both traditional design procedures (physically and numerically) and each of the SDW approaches, in order to optimise the quantity of data required and better understand the reliability of each method.

Overall, the data presented in this study implies that SDWs have the potential to be utilised effectively within specific parts of the design process. Assuming the 10% under-predictions observed in this work, it is likely that they would be best suited to early design stages to allow for more efficient sweeping of larger environmental conditions parameter space. However, if the method can be refined to provide an extreme load that is at least as conservative as the AoM of the ISS data then they may be appropriate for later design stages as well. For instance, in this study a relationship between a series of large waves and high surge responses is presented. Assuming that this relationship is transferable to alternative similar devices, this could potentially be exploited in the future to provide a more reliable surge extreme load, or optimise the number of runs required to further improve the efficiency of the method. Future work will also investigate any further relationships within the data to assess whether improvements can be made to the other responses presented in this study.

Author Contributions

S. Brown: conceptualisation, methodology, formal analysis, investigation, writing, visualisation. **T. Tosdevin**: conceptualisation, methodology, investigation, formal analysis, writing. **S. Jin**: conceptualisation, methodology, investigation. **M. Hann**: conceptualisation, methodology, writing. **D. Simmonds**: conceptualisation, supervision. **D. Greaves**: conceptualisation, funding acquisition, writing, supervision.

Acknowledgements

The authors acknowledge that this work was funded as part of the Engineering and Physical Sciences Research Council (EPSRC) project 'Supergen ORE Hub' [EP/S000747/1], with additional support from the 'Extreme Loading on Floating Offshore Wind Turbines (FOWTs) under Complex Environmental Conditions' project [EP/T004177/1].

References

Allen, C., Viselli, A., Dagher, H., Goupee, A., Gaertner, E., Abbas, N., Hall, M., Barter, G., 2020. Definition of the UMaine VolturnUS-S reference platform developed for the IEA Wind 15-Megawatt Offshore Reference Wind Turbine. Technical Report NREL/TP-5000-76773. Golden, CO: National Renewable Energy Laboratory. `https://www.nrel.gov/docs/fy20osti/76773.pdf`.

Brown, S., Greaves, D., Magar, V., Conley, D., 2016. Evaluation of turbulence closure models under spilling and plunging breakers in the surf zone. Coast. Eng. 114, 177–193.

Brown, S., Musiedlak, P.H., Ransley, E., Greaves, D., 2020. Quantifying the predictive capability of OpenFOAM 5.0: Focused wave impacts with floating bodies. International Journal of Offshore and Polar Engineering 30, 20–27.

Carleo, G., Cirac, I., Cranmer, K., Daudet, L., Schuld, M., Tishby, N., Vogt-Maranto, L., Zdeborová, L., 2019. Machine learning and the physical sciences. Reviews of Modern Physics 91, 045002.

Chen, L., Taylor, P., Draper, S., Wolgamot, H., Milne, I., Whelan, J., 2019. Response based design metocean conditions for a permanently moored fpso during tropical cyclones: Estimation of greenwater risk. Applied Ocean Research 89, 115–127.

Coe, R.G., Michelen, C., Eckert-Gallup, A., Sallaberry, C., 2018a. Full long-term design response analysis of a wave energy converter. Renewable Energy 116, 356–366.

Coe, R.G., Rosenberg, B.J., Quon, E.W., Chartrand, C.C., Yu, Y.H., Van Rij, J., Mundon, T.R., 2019. CFD design-load analysis of a two-body wave energy converter. Journal of Ocean Engineering and Marine Energy 5, 99–117.

Coe, R.G., Yu, Y.H., Van Rij, J., 2018b. A survey of WEC reliability, survival and design practices. Energies 11.

Dietz, J.S., 2005. Application of conditional waves as critical wave episodes for extreme loads on marine structures. Ph.D. thesis. Technical University of Denmark.

DNV, 2018. Floating wind turbine structures. Technical Report Dnvgl-st-0119. DNV GL.

Drummen, I., Wu, M., Moan, T., 2009. Numerical and experimental investigations into the application of response conditioned waves for long-term nonlinear analyses. Marine Structures 22, 576–593.

Edwards, E., Holcombe, A., Brown, S., Ransley, E., Hann, M., Greaves, D., 2023. Evolution of floating offshore wind platforms: A review of at-sea devices. Renewable and Sustainable Energy Reviews 183.

Gaertner, E., Rinker, J., Sethuraman, L., Zahle, F., Anderson, B., Barter, G., Abbas, N., Meng, F., Bortolotti, P., Skrzypinski, W., Scott, G., Feil, R., Bredmose, H., Dykes, K., Shields, M., Allen, C., Viselli, A., 2020. Definition of the IEA 15-Megawatt Offshore Reference Wind. Technical Report NREL/TP-5000-75698. Golden, CO: National Renewable Energy Laboratory. https://www.nrel.gov/docs/fy20osti/75698.pdf.

Global Wind Energy Council, 2022. Global offshore wind report 2022. URL: https://gwec.net/wp-content/uploads/2022/06/GWEC-Offshore-2022_update.pdf. last accessed: 6th Feb. 2023.

Göteman, M., Engström, J., Eriksson, M., Hann, M., Ransley, E., Greaves, D., Leijon, M., et al., 2015. Wave loads on a point-absorbing wave energy device in extreme waves, in: The Twenty-fifth International Ocean and Polar Engineering Conference, International Society of Offshore and Polar Engineers.

Grice, J., Taylor, P., Eatock Taylor, R., 2013. Near-trapping effects for multi-column structures in deterministic and random waves. Ocean Engineering 58, 60–77.

Hann, M., Greaves, D., Raby, A., 2015. Snatch loading of a single taut moored floating wave energy converter due to focussed wave groups. Ocean Engineering 96, 258–271.

Hann, M., Greaves, D., Raby, A., Howey, B., 2018. Use of constrained focused waves to measure extreme loading of a taut moored floating wave energy converter. Ocean Engineering 148, 33–42.

Haselsteiner, A.F., Coe, R.G., Manuel, L., Chai, W., Leira, B., Clarindo, G., Guedes Soares, C., Ásta Hannesdóttir, Dimitrov, N., Sander, A., Ohlendorf, J.H., Thoben, K.D., de Hauteclocque, G., Mackay, E., Jonathan, P., Qiao, C., Myers, A., Rode, A., Hildebrandt, A., Schmidt, B., Vanem, E., Huseby, A.B., 2021. A benchmarking exercise for environmental contours. Ocean Engineering 236, 109504.

Hersbach, H., Bell, B., Berrisford, P., Biavati, G., Horányi, A., Muñoz Sabater, J., Nicolas, J., Peubey, C., Radu, R., Rozum, I., Schepers, D., Simmons, A., Soci, C., Dee, D., Thépaut, J.N., 2018. Era5 hourly data on single levels from 1959 to present. Copernicus Climate Change Service Climate Data Store 10. doi:10.24381/cds.adbb2d47. (Accessed on 23-02-2023).

Holcombe, A., Edwards, E., Hann, M., Tosdevin, T., Greaves, D., 2023. A comparative study of potential-flow-based numerical models to experimental tests of a semisubmersible floating wind turbine platform, in: Proceedings of the 33rd International Ocean and Polar Engineering Conference, Ottawa, Canada.

IEC, 2016. Marine energy-wave, tidal and other water current converters-part 2: design requirements for marine energy systems. Technical Report 62600-2. International Electrotechnical Commission.

Jin, S., Brown, S., Tosdevin, T., Hann, M., Greaves, D., 2022. Laboratory investigation on short design wave extreme responses for floating hinged-raft wave energy converters. Frontiers in Energy Research 10. doi:https://doi.org/10.3389/fenrg.2022.1069108.

Katsidoniotaki, E., Nilsson, E., Rutgersson, A., Engström, J., Göteman, M., 2021. Response of point-absorbing wave energy conversion system in 50-years return period extreme focused waves. Journal of Marine Science and Engineering 9.

Li, L., Gao, Z., Moan, T., 2013. Joint environmental data at five european offshore sites for design of combined wind and wave energy devices, in: International Conference on Offshore Mechanics and Arctic Engineering, American Society of Mechanical Engineers. p. V008T09A006.

Li, Y., Fuhrman, D.R., 2021. Computational Fluid Dynamics Simulation of Deep-Water Wave Instabilities Involving Wave Breaking. Journal of Offshore Mechanics and Arctic Engineering 144. 021901.

Li, Y., Fuhrman, D.R., 2022. On the turbulence modelling of waves breaking on a vertical pile. Journal of Fluid Mechanics 953, A3.

Lin, Z., Qian, L., Bai, W., 2021. A coupled overset CFD and mooring line model for floating wind turbine hydrodynamics, in: Proceedings of the 31st International Ocean and Polar Engineering Conference, Rhodes, Greece.

Marino, E., Borri, C., Peil, U., 2011. A fully nonlinear wave model to account for breaking wave impact loads on offshore wind turbines. Journal of Wind Engineering and Industrial Aerodynamics 99, 483–490.

Michelen, C., Coe, R., 2015. Comparison of methods for estimating short-term extreme response of wave energy converters, in: OCEANS 2015-MTS/IEEE Washington, IEEE. pp. 1–6.

Ochi, M.K., 1998. Ocean Waves: The Stochastic Approach. Cambridge Ocean Technology Series, Cambridge University Press.

Palm, J., Eskilsson, C., Bergdahl, L., 2017. An hp-adaptive discontinuous Galerkin method for modelling snap loads in mooring cables. Ocean Engineering 144, 266 – 276.

Quon, E., Platt, A., Yu, Y.H., Lawson, M., 2016. Application of the most likely extreme response method for wave energy converters, in: ASME 2016 35th International Conference on Ocean, Offshore and Arctic Engineering, American Society of Mechanical Engineers Digital Collection.

Ransley, E., Brown, S., Edwards, E., Tosdevin, T., Monk, K., Reynolds, A., Greaves, D., Hann, M., 2022. Real time hybrid testing of a floating offshore wind turbine using a surrogate-based aerodynamic emulator, in: Proceedings of ASME 2022 International Offshore Wind Technical Conference, Boston, Massachusetts, US.

Ransley, E., Brown, S., Edwards, E., Tosdevin, T., Monk, K., Reynolds, A., Greaves, D., Hann, M., 2023. Real-time hybrid testing of a floating offshore wind turbine using a surrogate-based aerodynamic emulator. ASME Open Journal of Engineering .

Ransley, E., Brown, S., Hann, M., Greaves, D., Windt, C., Ringwood, J., Davidson, J., Schmitt, P., Yan, S., Wang, J.X., Wang, J.H., Ma, Q., Xie, Z.H., Giorgi, G., Hughes, J., Williams, A., Masters, I., Lin, Z., Chen, H., Qian, L., Ma, Z., Causon, D., Mingham, C., Chen, Q., Ding, H., Zang, J., van Rij, J., Yu, Y., Tom, N., Li, Z., Bouscasse, B., Ducrozet, G., Bingham, H., 2020a. A blind comparative study of focused wave interactions with floating structures (CCP-WSI Blind Test Series 2). Proceedings of the Institution of Civil Engineers - Engineering and Computational Mechanics 174, 46–61.

Ransley, E., Yan, S., Brown, S., Hann, M., Graham, D., Windt, C., Schmitt, P., Davidson, J., Ringwood, J., Musiedlak, P.H., et al., 2020b. A blind comparative study of focused wave interactions with floating structures (CCP-WSI Blind Test Series 3). International Journal of Offshore and Polar Engineering 30, 1–10.

Ropero-Giralda, P., Crespo, A.J., Tagliafierro, B., Altomare, C., Domínguez, J.M., Gómez-Gesteira, M., Viccione, G., 2020. Efficiency and survivability analysis of a point-absorber wave energy converter using DualSPHysics. Renewable Energy 162, 1763–1776.

Rosenberg, B.J., Mundon, T.R., Coe, R.G., Quon, E.W., Chartrand, C.C., Yu, Y.H., Van Rij, J.A., 2019. Development of WEC design loads: A comparison of numerical and experimental approaches. Technical Report. National Renewable Energy Lab.(NREL), Golden, CO (United States).

Tang, S., Sweetman, B., Gao, J., 2021. Nonlinear effects and dynamic coupling of floating offshore wind turbines using geometrically-exact blades and momentum-based methods. Ocean Engineering 229, 108866.

Taylor, P.H., Jonathan, P., Harland, L.A., 1997. Time domain simulation of jack-up dynamics with the extremes of a gaussian process. Journal of Vibration and Acoustics 119, 624–628.

Tosdevin, T., Jin, S., Cao, A., Simmonds, D., Hann, M., , Greaves, D., 2021. Extreme responses of a hinged raft type wave energy convertor, in: Proceedings of the 14th European Wave and Tidal Energy Conference, Plymouth, UK.

Tosdevin, T., Jin, S., Simmonds, D., Hann, M., Greaves, D., 2022. On the use of constrained focused waves for characteristic load prediction, in: Proceedings of the 5th International Conference on Renewable Energies Offshore (RENEW), Lisbon, Portugal.

Tromans, P.S., Anaturk, A.R., Hagemeijer, P., et al., 1991. A new model for the kinematics of large ocean waves-application as a design wave, in: The first international offshore and polar engineering conference, International Society of Offshore and Polar Engineers.

Van Rij, J., Yu, Y.H., Coe, R.G., 2018. Design load analysis for wave energy converters, in: International Conference on Offshore Mechanics and Arctic Engineering, American Society of Mechanical Engineers. p. V010T09A031.

Van Rij, J., Yu, Y.H., Guo, Y., Coe, R.G., 2019. A wave energy converter design load case study. Journal of Marine Science and Engineering 7, 250.

Viselli, A.M., Forristall, G.Z., Pearce, B.R., Dagher, H.J., 2015. Estimation of extreme wave and wind design parameters for offshore wind turbines in the gulf of maine using a pot method. Ocean Engineering 104, 649–658. doi:https://doi.org/10.1016/j.oceaneng.2015.04.086.

Wang, L., Jonkman, J., Hayman, G., Platt, A., Jonkman, B., Robertson, A., 2022. Recent hydrodynamic modeling enhancements in openfast, in: 4th International Offshore Wind Technical Conference (IOWTC2022), Boston, Massachusetts. URL: https://www.nrel.gov/docs/fy23osti/83679.pdf. report: NREL/CP-5000-83679.

Wang, S., Larsen, T.J., Bredmose, H., 2021. Ultimate load analysis of a 10 MW offshore monopile wind turbine incorporating fully nonlinear irregular wave kinematics. Marine Structures 76, 102922.

Zhou, Y., Xiao, Q., Peyrard, C., Pan, G., 2021. Assessing focused wave applicability on a coupled aero-hydro-mooring fowt system using cfd approach. Ocean Engineering 240, 109987. URL: https://www.sciencedirect.com/science/article/pii/S0029801821013275, doi:https://doi.org/10.1016/j.oceaneng.2021.109987.